frontiers in Chemistry

ORIGINAL RESEARCH
published: 16 October 2018
doi: 10.3389/fchem.2018.00469

A Versatile Polyoxovanadate in Diverse Cation Matrices: A Supramolecular Perspective

*Srinivasa Rao Amanchi and Samar K. Das**

School of Chemistry, University of Hyderabad, Central University, Hyderabad, India

A series of decavanadate based compounds, formulated as $[Co(H_2O)_6][\{Na_4(H_2O)_{14}\}\{V_{10}O_{28}\}]\cdot 4H_2O$ (**1**), $[Zn(H_2O)_6][Na_3(H_2O)_{14}]$ $[HV_{10}O_{28}]\cdot 4H_2O$ (**2**), $[HMTAH]_2$ $[\{Zn(H_2O)_4\}_2\{V_{10}O_{28}\}]\cdot 2H_2O$ (**3**), $[\{Co(3\text{-amp})(H_2O)_5\}]_2$ $[3\text{-ampH}]_2$ $[V_{10}O_{28}]\cdot 6H_2O$ (**4**), $[4\text{-ampH}]_{10}[\{Na(H_2O)_6\}\{HV_{10}O_{28}\}][V_{10}O_{28}]\cdot 15H_2O$ (**5**), $[\{4\text{-ampH}\}_6\{Co(H_2O)_6\}_3][V_{10}O_{28}]_2\cdot 14H_2O$ (**6**), and $[\{4\text{-ampH}\}_{10}\{Zn(H_2O)_6\}][V_{10}O_{28}]_2\cdot 10H_2O$ (**7**), have been synthesized (where HMTAH = mono-protonated hexamethylenetetramine, 3-ampH = protonated 3-amino pyridine and 4-ampH= protonated 4-aminopyridine) from the relevant aqueous sodium-vanadate solution, by varying the pH of the solution and amino pyridine/hexamine derivatives as well as transition metal salts (Co(II)- and Zn(II)-salts). In this series of compounds **1**–**7**, the polyoxovanadate (POV) cluster $[V_{10}O_{28}]^{6-}$ is the common cluster anion, stabilized by diverse cations. The diverse supramolecular patterns around the decavanadate cluster anion in different cationic matrices have been described to understand the microenvironment in the decavanadate-based minerals. All of these compounds have solvent water molecules in their respective crystal lattices. Since water can interact directly with cations and anions, providing an additional stability and structural diversity, we have analyzed supramolecular water structures in all these compounds to comprehend the role of the lattice water in the formation of natural decavanadate containing minerals. Compounds **1**–**7**, that are isolated at an ambient condition from aqueous solution, are characterized by routine spectral analysis, elemental analyses and finally unambiguously by single crystal X-ray crystallography.

Keywords: decavanadate cluster anion, diverse cations, crystal structures, supramolecular chemistry, decavanadate mineralogy

OPEN ACCESS

Edited by:
Debbie C. Crans,
Colorado State University,
United States

Reviewed by:
Akira Odani,
Kanazawa University, Japan
Tilo Söhnel,
University of Auckland, New Zealand
Enrique González-Vergara,
Benemérita Universidad Autónoma de Puebla, Mexico

****Correspondence:***
Samar K. Das
skdas@uohyd.ac.in

Specialty section:
This article was submitted to Inorganic Chemistry, a section of the journal Frontiers in Chemistry

Received: *30 April 2018*
Accepted: *18 September 2018*
Published: *16 October 2018*

Citation:
Amanchi SR and Das SK (2018) A Versatile Polyoxovanadate in Diverse Cation Matrices: A Supramolecular Perspective. Front. Chem. 6:469. doi: 10.3389/fchem.2018.00469

INTRODUCTION

The modern chemical research on polyoxometalates (POMs)-based solid state materials fascinates synthetic chemists because of their potential applications in diverse research areas, such as, catalysis (Vazylyev et al., 2005; Hill, 2007; Zhou et al., 2014; Lechner et al., 2016; Mukhopadhyay et al., 2018), medicinal chemistry (Pope and Müller, 1991; Liu et al., 2012; Xie et al., 2018), and materials science (Guo et al., 2000; Rao et al., 2011; Kulikov and Meyer, 2013; Omwoma et al., 2015; Walsh et al., 2016). Among these, the area of polyoxovanadate (henceforth, POV) based materials have received special attention due to not only their diverse topologies (Miiller et al., 1990; Klemperer et al., 1992; Chen et al., 2005), structural (Miiller et al., 1987; Koene et al., 1999) and electronic properties (Müller et al., 1997) but also their fascinating versatile industrial applications, e.g., catalysis (Gao and Hua, 2006) and materials applications (Khan et al., 2003; Arumuganathan and Das, 2009; Chen et al., 2018). Among POVs, decavanadate cluster anion $[V_{10}O_{28}]^{6-}$ is a versatile POM cluster

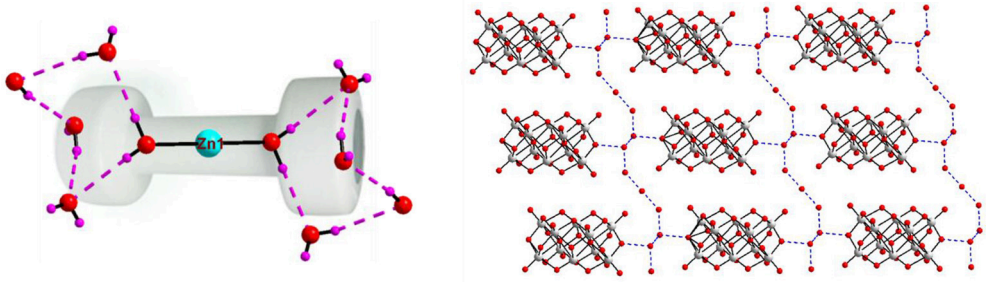

GRAPHICAL ABSTRACT | Decavanadate cluster $\{V_{10}O_{28}\}^{6-}$ is the common anion to synthesize the materials **1–7**, ranging from discrete compounds to coordination polymers. Water clusters, such as, cyclic pentamers are established in some of the crystal structures due to water-water hydrogen bonding (O–H···O) interactions. There are analogies between these synthesized compounds and decavanadate based minerals in terms of the microenvironment around the isopolyanion.

anion, which is constructed by ten edge-shared VO_6 octahedra with D_{2h} symmetry (**Figure 1**). Eight terminals-, fourteen doubly bridged (μ^2)-, four triply bridged (μ^3)- and two hexa bridged (μ^6)-oxygen atoms exist within this $[V_{10}O_{28}]^{6-}$ cluster anion. Numerious decavanadate based compounds are known in literature (Crans et al., 2017; Naslhajian et al., 2017; Yerra and Das, 2017) where the decavanadate cluster anion has been isolated using diverse cations including transition metal- and alkali metal-coordination complex cations; relevant supramolecular chemistry has also been described in the context of POV based materials chemistry (Sánchez-Lombardo et al., 2014; Wang et al., 2016). Choosing a particular cation plays a vital role in tuning the property of the resulting decavanadate cluster containing ion pair compound (Chatkon et al., 2013). The biological role of decavanadate cluster is enormous (Rehder, 2013; Winkler et al., 2017). Aureliano and co-workers described, in a perspective, the biological interactions of decavanadate with ion pump Ca^{2+}-ATPase and compared the mode of action with those of already established ion-pump inhibitors of therapeutic importance (Aureliano et al., 2013). In addition to ion pumps, lipid structures also have been shown to represent biological targets for decavanadate (Aureliano and Crans, 2009). Crans and co-workers reported that rabbit skeletal muscle phosphorylase can be inhibited by decavanadate (Crans et al., 2004). They examined the interactions of decavanadate in an inorganic model system as well as in cells and determined the biological effects of decavanadate on rat basophilic leukemia (RBL-2H3) plasma membrane functions (Al-Qatati et al., 2013). In a recent report, de Carvalho and co-workers have demonstrated that decavanadate can interact with G-actin (multifunctional proteins), activating a protein conformational change and thereby that induces oxidation of the cysteine core residues (Marques et al., 2017). Even though, a good number of reports of the decavanadate cluster anion on diverse aspects of its biological significance is available including its catalytic applications (Kwon et al., 1988; Villa et al., 2001; Derat et al., 2006; Conte and Floris, 2010; Mestiri et al., 2013; Martín-Caballero et al., 2016; Amini et al., 2017; Huang et al., 2018), there are only few reports on decavanadate-based inorganic compounds along with their structural characterizations, that have been used as models to understand the formation of decavanadate-based minerals in Nature. D. C. Crans and C. C. McLauchlan and their co-workers have recently published an excellent review article covering the mineral-aspects of decavanadate compounds (Crans et al., 2017). There are more than 10 such minerals known, where the negative charges of decavanadate anion are counter-balanced mostly by alkali and alkali-earth metal cations and these minerals are stabilized with a good number of solvent water molecules. In order to comprehend their speciation in Nature, inorganic chemists have to synthesize decavanadate-based compounds with diverse cations from an aqueous solution and to characterize them crystallographically to investigate the micro-environments around decavanadate anion in these diverse cation matrices. This might offer an understanding the formation of decavanadate-based minerals in Nature. Moreover, exploration of the detailed interactions between decavanadate cluster anion and diverse counter cations is not only important for their categorization (da Silva et al., 2003) but also to gain the knowledge of new supramolecular chemistry of decavanadate ion (Crans et al., 1994; Yi et al., 2010; Chatkon et al., 2014). Thus we have synthesized and structurally characterized seven decavanadate based ion-pair compounds $[Co(H_2O)_6][\{Na_4(H_2O)_{14}\}\{V_{10}O_{28}\}]\cdot 4H_2O$ (**1**), $[Zn(H_2O)_6]\ [Na_3(H_2O)_{14}]\ [HV_{10}O_{28}]\cdot 4H_2O$ (**2**), $[HMTAH]_2[\{Zn(H_2O)_4\}_2\{V_{10}O_{28}\}]\cdot 2H_2O$ (**3**), $[\{Co(3\text{-amp})(H_2O)_5\}_2[3\text{-ampH}]_2[V_{10}O_{28}]\cdot 6H_2O$ (**4**), $[4\text{-ampH}]_{10}[\{Na(H_2O)_6\}\ \{HV_{10}O_{28}\}][V_{10}O_{28}]\ \cdot 15H_2O$ (**5**), $[\{4\text{-ampH}\}_6\{Co(H_2O)_6\}_3][V_{10}O_{28}]_2\cdot 14H_2O$ (**6**), and $[\{4\text{-ampH}\}_{10}\{Zn(H_2O)_6\}][V_{10}O_{28}]_2\ \cdot 10H_2O$ (**7**). Since in the present work, we are dealing with diverse cations ion-pairing with a common decavanadate polyanion, diverse supramolecular interactions are possible in their respective crystal structures. We have analyzed here the detailed supramolecular chemistry associated with each of these compounds and we have compared the microenvironment of decavanadate anion in these synthesized systems with that in some of the known decavanadate-based natural minerals (**Graphical Abstract**).

EXPERIMENTAL SECTION

Materials

Sodium metavanadate was received from SISCO Laboratory. The distilled water was used throughout the experiments.

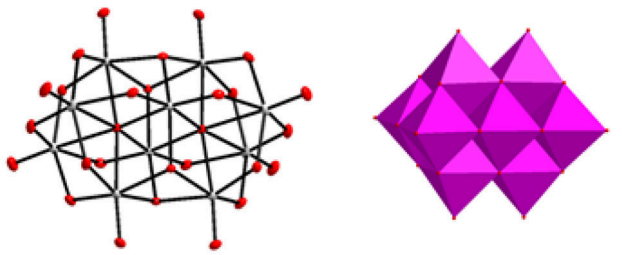

FIGURE 1 | Decavanadate cluster $[V_{10}O_{28}]^{6-}$ described in ball and stick and polyhedral representations respectively.

2-Aminopyridine, 3-aminopyridine, 4-aminopyridine, and hexamine (hexamethylenetetramine) were received from CHEMLABS. $Zn(NO_3)_2{\cdot}6H_2O$ and $Co(NO_3)_2{\cdot}6H_2O$ were used as received from S.D. Fine and FINAR chemicals respectively.

Physical Measurements

Micro analytical (C, H, N) data were obtained with a FLASH EA 1112 Series CHNS Analyzer. Infrared (IR) spectra were recorded on KBr pellets with a JASCO FT/IR-5300 spectrometer in the region of 400–4000 cm^{-1}.

Preparation of Compounds 1–7

Synthesis of $[Co(H_2O)_6][\{Na_4(H_2O)_{14}\}\{V_{10}O_{28}\}]{\cdot}4H_2O$ (1)

Sodium metavanadate (1 g, 4.13 mmol) was dissolved in 100 mL of water and its pH was adjusted to 9.0 by dil. HCl. In a separate beaker, the metal salt, $Co(NO_3)_2{\cdot}6H_2O$ (0.5 g, 1.7 mmol) was dissolved in 20 mL of water. This reaction mixture of metal salt was added drop wise to the sodium vanadate solution with stirring. The resulting reaction mixture was stirred for 5 h (during stirring, the formation of precipitate / turbidity was dissolved by heating the reaction mixture at 70–80°C in three to four slots). The reaction mixture was then filtered and kept in open beaker for crystallization without any disturbance at room temperature. After 1 week, orange colored crystals formed, were filtered, washed with plenty of water and finally dried at room temperature. One of the single crystals, suitable for X-ray diffraction study, was selected and characterized structurally. Yield: 1.23 g. Anal. Calcd. (%) for $CoH_{48}Na_4O_{52}V_{10}$:. C, 0.00; H, 3.14, N, 0.00. Found: C, 0.03; H, 3.39, N, 0.04. IR (KBr pellet): (ν/cm^{-1}) 3329, 3171, 1658, 1622, 1541, 1475, 1383, 1327, 1244, 1168, 991, 889, 829, 765, 617.

Synthesis of $[Zn(H_2O)_6][Na_3(H_2O)_{14}][HV_{10}O_{28}]{\cdot}4H_2O$ (2)

The reaction procedure is same as the synthesis of compound **1** except $Zn(NO_3)_2{\cdot}6H_2O$ (0.5 g, 1.68 mmol) was taken instead of $Co(NO_3)_2{\cdot}6H_2O$. The resulting reaction mixture was stirred for 5 h (during stirring, the formation of precipitate / turbidity was dissolved by heating the reaction mixture at 70–80°C in three to four slots). The reaction mixture was then filtered and kept in open beaker for crystallization without any disturbance at room temperature. After 1 week, orange colored crystals formed, were filtered, washed with plenty of water and finally dried at room temperature. One of the single crystals from, suitable for X-ray diffraction study, was selected and characterized structurally. Yield: 0.35 g. Anal. Calcd. (%) for $H_{58}Na_3O_{52}V_{10}Zn$: C, 0.00; H, 3.81; N, 0.00. Found: C, 0.09; H, 3.71; N 0.10. IR (KBr pellet): (ν/cm^{-1}) 3337, 3229, 3057, 2085, 1614, 1560, 1485, 1398, 1327, 1332, 1280, 1072,922, 885, 829, 679, 584.

Synthesis of $[HMTAH]_2[\{Zn(H_2O)_4\}_2\{V_{10}O_{28}\}]{\cdot}2H_2O$ (3)

Sodium metavanadate (1 g, 4.13 mmol) was dissolved in 100 mL of water and its pH was adjusted to 3.0 by dil. HCl. In a separate beaker, the $Zn(NO_3)_2{\cdot}6H_2O$ and hexamine (0.25 g, 1.68 mmol) were dissolved in 20 mL of water. This reaction mixture was added drop wise to the sodium vanadate solution with stirring. The resulting reaction mixture was stirred for 5 h (during stirring, the formation of precipitate / turbidity was dissolved by heating the reaction mixture at 70–80°C in three to four slots). The reaction mixture was then filtered and kept in open beaker for crystallization without any disturbance at room temperature. After 1 week, orange colored crystals formed, were filtered, washed with water and finally dried at room temperature. Yield: 0.27 g. Anal. Calcd. (%) for $Zn_2V_{10}O_{38}C_{12}N_8H_{46}$: C, 9.29; H, 2.99; N, 7.23. Found: C, 9.11; H, 2.78; N, 7.89. IR (KBr pellet): (ν/cm^{-1}) 3420, 3310, 3190, 3078, 2918, 1647, 1614, 1570, 1464, 1386, 1313, 1230, 1182, 1086, 920, 883, 605.

Synthesis of $[\{Co(3\text{-amp})(H_2O)_5\}]_2[3\text{-ampH}]_2[V_{10}O_{28}]{\cdot}6H_2O$ (4)

Sodium metavanadate (1 g, 4.13 mmol) was dissolved in 100 mL of water and its pH was adjusted to 3.0 by dil. HCl. In a separate beaker, the $Co(NO_3)_2{\cdot}6H_2O$ (0.5 g, 1.7 mmol) and 3-aminopyridine (0.25 g, 1.68) were dissolved in 20 mL of water. This reaction mixture was added drop wise to the sodium vanadate solution with stirring. The resulting reaction mixture was stirred for 5 h (during stirring, the formation of precipitate/turbidity was dissolved by heating the reaction mixture at 70–80°C in three to four slots). The reaction mixture was then filtered and kept in open beaker for crystallization without any disturbance at room temperature. After 1 week, orange colored crystals formed, were filtered, washed with water and finally dried at room temperature. Yield: 0.27 g. Anal. Calcd. (%) for $Co_2V_{10}O_{44}C_{20}N_8H_{58}$: C, 13.79; H, 3.36; N, 6.43. Found: C, 13.21; H, 3.23; N, 6.89. IR (KBr Pellet): (ν/cm^{-1}): 3456, 3322, 3170, 2998, 2978, 1654, 1625, 1567, 1469, 1398, 1267, 1156, 1076, 937, 896, 608.

Synthesis of $[4\text{-ampH}]_{10}[\{Na(H_2O)_6\}\{HV_{10}O_{28}\}][V_{10}O_{28}]{\cdot}15H_2O$ (5)

Sodium metavanadate (1 g, 4.13 mmol) was dissolved in 100 mL of water and its pH was adjusted to 6.0 by dil. HCl. In a separate beaker, the 4-aminopyridine (0.25 g, 1.70 mmol)

were dissolved in 20 mL of water. 4-aminopyridine solution was added drop wise to the sodium vanadate solution with stirring. The resulting reaction mixture was stirred for 5 h (during stirring, the formation of precipitate / turbidity was dissolved by heating the reaction mixture at 70–80°C in three to four slots). The reaction mixture was then filtered and kept in an open beaker for crystallization without any disturbance at room temperature. After 1 week, orange colored crystals formed, were filtered, washed with good amount of water and finally dried at room temperature. Yield: 0.47 g. Anal. Calcd (%) for $V_{20}NaO_{77}C_{50}N_{20}H_{113}$: C, 18.37; H, 3.48; N, 8.57. Found: C, 18.15; H 3.99; N, 8.55. IR (KBr Pellet): (ν/cm^{-1}): 3467, 3335, 3178, 2929, 1684, 1629, 1547, 1498, 1339, 1235, 1178, 1007, 967, 849, 619.

Synthesis of $[\{4\text{-ampH}\}_6\{Co(H_2O)_6\}_3][V_{10}O_{28}]_2\cdot 14H_2O$ (6)

Synthesis of compound **6** is same as that of compound **4** except 4-aminopyridine (0.25 g, 1.68 mmol) was taken (instead of 3-aminopyridine) in the reaction and maintained the same pH as was maintained in the synthesis of compound **4**. The resulting reaction mixture was stirred for 5 hrs (during stirring, the formation of precipitate / turbidity was dissolved by heating the reaction mixture at 70–80°C in three to four slots). The reaction mixture was then filtered and kept in open beaker for crystallization without any disturbance at room temperature. After 1 week, orange colored crystals formed, were filtered, washed with water and finally dried at room temperature. Yield: 1.87 g. Anal. Calcd. (%) for $V_{20}Co_3O_{88}C_{30}N_{12}H_{106}$: C,11.13; H, 3.30; N, 5.19. Found: C, 11.55; H, 3.79; N, 5.43. IR (KBr pellet) (ν/cm^{-1}): 3427, 3345, 3196, 2822, 1690, 1645, 1556, 1489, 1338, 1268, 1189, 1039, 979, 890, 650.

Synthesis of $[\{4\text{-ampH}\}_{10}\{Zn(H_2O)_6\}][V_{10}O_{28}]_2\cdot 10H_2O$ (7)

Synthesis of compound **7** is same as that of compound **4** except $Zn(NO_3)_2\cdot 6H_2O$ (0.5 g, 1.7 mmol) and 4-aminopyridine (0.25 g, 2.6 mmol) were taken (instead of $Co(NO_3)_2\cdot 6H_2O$ and 3-aminopyridine respectively) in the reaction and maintained the same pH as was maintained in the synthesis of compound **4**. The resulting reaction mixture was stirred for 5 h (during stirring, the formation of precipitate/turbidity was dissolved by heating the reaction mixture at 70–80°C in

TABLE 1 | Crystal data and structure refinement details for compounds **2**, **3**, and **4**.

Entry	2	3	4
Molecular formula	$H_{10}ZnNa_3O_{52}V_{10}$	$C_{12}H_{24}N_8O_{38}V_{10}Zn_2$	$C_{20}H_{38}Co_2N_8O_{44}V_{10}$
Formula weight	1485.42	1528.53	1721.84
Temperature (K)	298 (2)	298 (2)	298 (2)
Wavelength (Å)	0.71073	0.71073	0.71073
Crystal system	Triclinic	Monoclinic	Triclinic
Space group	*P*-1	*P21/c*	*P-1*
a (Å)	8.940 (3)	10.5993 (17)	10.5180 (16)
b (Å) 13.877 (4)	16.4355 (18)	11.9208 (18)	
c (Å)	18.360 (5)	13.865 (3)	12.711 (2)
α (deg)	91.766 (4)	90.00	97.818 (2)
β (deg) 91.744 (4)	120.191 (13)	107.937 (2)	
γ (deg)	104.705 (4)	90.00	100.240 (2)
Volume (Å^3) 2200.4 (11)	2087.7 (6)	1460.8 (4)	
Z	2	2	1
ρ (g cm^{-3})	2.243	2.432	1.957
μ (mm^{-1}) 2.718		3.378	2.181
F (000)	1438	1492	850
Crystal size (mm^3)	0.24 × 0.18 × 0.14	0.36 × 0.18 × 0.14	0.46 × 0.34 × 0.20
θ range (°)	1.11 to 25.00	2.98 to 25.00	2.20 to 25.09
Reflections collected	18286	9787	13958
Unique reflections	6532	3683	5139
R(int)	0.0238	0.0819	0.0209
Parameters	7714/0 /640	3683/0/316	5139/0/455
Goodness of fit on F^2	1.063	1.086	1.537
R_1, wR_2 [I > 2 sigma(I)]	0.0433, 0.1238	0.0885, 0.2660	0.0465,0.1582
R_1, wR_2 (all data)	0.0511, 0.1300	0.1387,0.2895	0.0479, 0.1598
Largest diff. Peak and hole (e.Å^{-3})	0.989/−1.051	1.854, −3.604	2.248, −0.840

three to four slots). The reaction mixture was then filtered and kept in open beaker for crystallization without any disturbance at room temperature. After 1 week, orange colored crystals formed, were filtered, washed thoroughly with water and finally dried at room temperature. One of the single crystals, suitable for X-ray diffraction study, was selected and characterized structurally. The product obtained with Yield of 1.47 g. Anal. Calcd (%) for $V_{20}ZnO_{72}C_{50}N_{20}H_{102}$: C, 18.65; H, 3.19; N, 8.70. Found: C, 18.32; H, 3.45; N, 8.63. IR (KBr pellet) (ν/cm^{-1}): 3445, 3385, 3187, 2842, 1677, 1649, 1537, 1424, 1373, 1229, 1175, 1038, 929, 885, 643.

TABLE 2 | Crystal data and structure refinement details for compounds **5, 6,** and **7**.

Entry	5	6	7
Molecular formula	$C_{50}H_{100}N_{20}NaO_{72}V_{20}$	$C_{30}H_{88}Co_3N_{12}O_{88}V_{20}$	$C_{50}H_{96}N_{20}O_{72}V_{20}Zn$
Formula weight	3175.29	3220.71	3213.64
Temperature (K)	298 (2)	100 (2)	100 (2)
Wavelength (Å)	0.71073	0.71073	0.71073
Crystal system	Monoclinic	Triclinic	Monoclinic
Space group	*P21/c*	*P*-1	*P*2 (1)/c
a (Å)	13.1158 (10)	10.5396 (12)	13.087 (3)
b (Å)	20.0118 (16)	11.4041 (13)	19.997 (4)
c (Å)	20.1107 (16)	21.068 (2)	20.005 (4)
α(°)	90.000	99.843 (2)	90.000
β (°)	95.7520 (10)	91.015 (2)	95.680 (3)
γ(°)	90.000	91.547 (2)	90.000
Volume ($Å^3$)	5251.9 (7)	2493.5 (5)	5209.6 (18)
Z	2	1	2
ρ (g cm^{-3})	2.008	2.145	2.049
μ (mm^{-1})	1.808	2.387	2.043
F (000)	3174	1597	3204
Crystal size (mm^3)	0.36 × 0.24 × 0.18	0.34 × 0.18 × 0.16	0.26 × 0.20 × 0.18
θ range (°)	1.44 to 26.01	2.20 to 26.00	1.44 to 26.02
Reflections collected	54039	25672	50931
Unique reflections	10321	9682	10234
R(int)	0.0318	0.0230	0.0476
Parameters	10321/0/936	9682/0/898	10234/0/832
GOF on F^2	1.025	1.188	1.147
R_1, $wR_2[I > 2\sigma(I)]$	0.0355, 0.0962	0.0465, 0.1044	0.0468, 0.1020
R_1, wR_2 (all data)	0.0406, 0.0997	0.0500, 0.1060	0.0549, 0.1056
Largest diff. Peak and hole (e.$Å^{-3}$)	2.108, −0.417	2.084 and −1.072	0.551, −0.345

TABLE 3 | Decavanadate-based minerals.

Name of minerals	Formulas	Type of decavanadate	References
Huemulite	$Na_4\ Mg(V_{10}O_{28})\bullet 24H_2O$	Oxidized	Colombo et al., 2011
Hughesite	$Na_3Al(V_{10}O_{28})\bullet 22H_2O$	Oxidized	Rakovan et al., 2011
Hummerite	$K_2Mg_2(V_{10}O_{28})\bullet 16H_2O$	Oxidized	Hughes et al., 2002
Kokinosite	$Na_2Ca_2(V_{10}O_{28})\bullet 24H_2O$	Oxidized	Kampf et al., 2014
Lasalite	$Na_2Mg_2\ (V_{10}O_{28})\bullet 20H_2O$	Oxidized	Hughes et al., 2008
Magnesiopascoite	$MgCa_2(V_{10}O_{28})\bullet 16H_2O$	Oxidized	Kampf and Steele, 2008
Pascoite	$Ca_3(V_{10}O_{28})\bullet 17H_2O$	Oxidized	Hughes et al., 2005
Postite	$MgAl_2(V_{10}O_{28})(OH)_2\bullet 27H_2O$	Oxidized	Kampf et al., 2012
Schindlerite	$Na_2(H_3O)_4(V_{10}O_{28})\bullet 10H_2O$	Oxidized	Kampf et al., 2013b
Wernerbaurite	$Ca_2(H_3O)_2(V_{10}O_{28})\bullet 16H_2O$	Oxidized	Kampf et al., 2013b
Gunterite	$Na_4(H_2V_{10}O_{28})\bullet 22H_2O$	Protonated	Kampf et al., 2011b
Rakovanite	$Na_3(H_3V_{10}O_{28})\bullet 15H_2O$	Protonated	Kampf et al., 2011a
Nashite	$Na_3Ca_2[(V^{IV}V^{V}_9)O_{28}]\bullet 24H_2O$	Mixed valent	Kampf et al., 2013a

X-ray Data Collection and Structure Determination

Data were measured on a Bruker SMART APEX CCD area detector system [λ(Mo Kα) = 0.71073 Å] with a graphite monochromator. 2400 frames were recorded with an ω scan width of 0.3°, each for 8 s keeping a crystal detector distance of 60 mm with a collimator of 0.5 mm. The data were reduced using SAINTPLUS program (software for the CCD detector system, Bruker Analytical X-ray Systems Inc., Madison, WI, 1998); the structures were solved using SHELXS-97 (Sheldrick, 1997) and refined using SHELXL-97 (Sheldrick, 1997). All non hydrogen atoms were refined anisotropically. We tried to locate the hydrogen atom of solvent water molecules for compound **2** through differential Fourier maps, but couldn't succeed. A summary of the crystallographic data and structure determination parameters are described in **Table 1** for compounds **1–2**, in **Table 2** for compounds **3–5** and in **Table 3** for compounds **6** and **7**. Bond lengths and angles for decavanadate anionic cluster for **1** (as it is common cluster for all compounds) are provided in **Table S1** they are in good agreement with those of reported decavanadate cluster anion $[V_{10}O_{28}]^{6-}$ (Rao et al., 2011). CCDC- 1840294 (for compound **3**), - 1840295 (for compound **4**), - 1840296 (for compound **5**), - 1840297 (for compound **6**) and - 1840298 (for compound **7**) contain the supplementary crystallographic data for this paper. These data can be obtained free of charge from The Cambridge Crystallographic Data Center via www.ccdc.cam.ac.uk/ data_request/cif. CSD-434511 contains the supplementary crystallographic data for carbon free compound **2**; the details of the relevant crystal structure investigation may be obtained from the Fachinformationszentrum, Karlsruhe, D-76344 Eggenstein-Leopoldshafen, Germany (fax: (+49) 7247-808-666; e-mail: crysdata@fiz-karlsruhe.de) on quoting the depository number CSD-434511. Compound **1** (CSD 418030) is already structurally reported compound.

RESULTS AND DISCUSSION

Synthesis

The synthetic method for the title compounds is simple one pot wet synthesis at a moderate temperature and their isolations are dependent on pH of the concerned solutions. Formation of the decavanadate cluster is feasible in the pH range of 2–9 in the solution, where pH of the solution is maintained by adding dil. HCl acid. Here, we have isolated seven ion pair compounds by altering the various cations and simultaneously pH condition. The formation of decavanadate cluster anion can be explained by protonation of vanadate anion and followed by a series of condensation reactions. The overall chemical reaction for the formation of decavanadate anion is given in equation 1. As expected, IR spectra of all these synthesized compounds reveal the presence of decavanadate anionic cluster as a common anionic component in title compounds. Vanadium-oxygen IR stretching frequencies of the decavanadate cluster anion containing ion pair compound depends on the type of the cation, associated with the anion.

$$10VO_3^- + 4H^+ \rightarrow [V_{10}O_{28}]^{6-} + 2H_2O \quad (1)$$

Generaly, decavanadate cluster anion decomposes to tetravanadate above pH 7. We still could isolate compounds **1** and **2** at a higher pH value (more than pH 7). We believe that, in our synthesis, although the starting PH is in the range of 9-10, it drops down when the salts are added. That is why, we could isolate decavanadate from the reaction mixture.

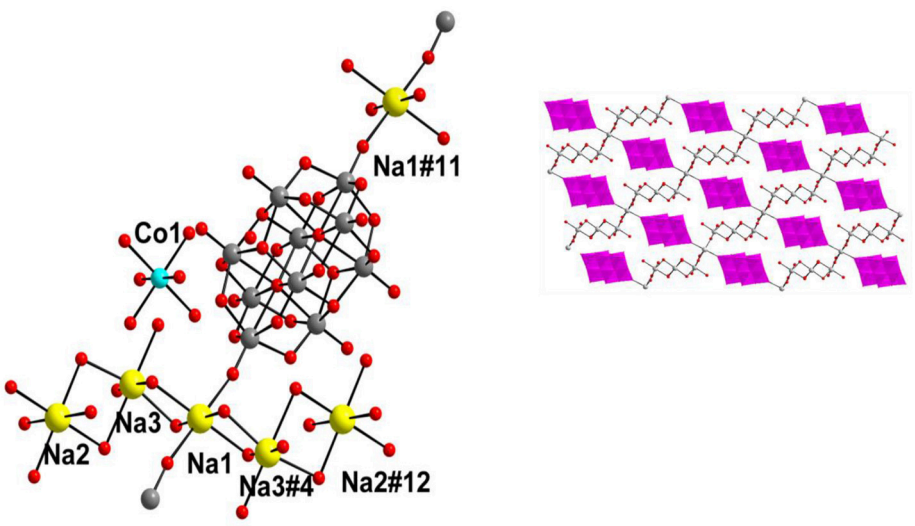

FIGURE 2 | Left: Ball and stick representation of total molecule of the $[Co(H_2O)_6][\{Na_4(H_2O)_{14}\}\{V_{10}O_{28}\}]\cdot 4H_2O$ (**1**) (Hydrogen atoms and solvent water molecules are omitted for clarity). color codes: Co, cyan; Na, yellow; O, red; V, light grey. **Right:** two-dimensional coordination polymer, formed in the crystal structure of compound **1**. Decavanadate clusters are shown in polyhedral representation (with pink color).

Molecular Structures and Supramolecular Chemistry

Compound $[Co(H_2O)_6][\{Na_4(H_2O)_{14}\}\{V_{10}O_{28}\}]\cdot 4H_2O$ (1)

The synthesis and crystal structure of compound **1** has already been reported (Mestiri et al., 2013). Even then, we have described the crystal structure of compound **1** here in terms of supramolecular chemistry. The asymmetric unit of compound **1** reveals the presence of half of the decavanadate cluster, which supports the sodium-aqua-cluster complex cation $\{Na_2(H_2O)_7\}^{2+}$ by a coordinate covalent bond and an uncoordinated cobalt tri-aqua complex acting as the cation along with two lattice water molecules. The cationic species $\{Na_2(H_2O)_7\}^{2+}$ consists of three crystallographically independent sodium atoms, namely a Na3 (full occupancy), a Na2 (half occupancy) and a Na1 (half occupancy) in the asymmetric unit, which also includes the cobalt atom in the special position. Accordingly the full molecule is formulated as $[Co(H_2O)_6][\{Na_4(H_2O)_{14}\}\{V_{10}O_{28}\}]\cdot 4H_2O$ (**1**). Thus, in compound **1**, the negative charges of $\{V_{10}O_{28}\}^{6-}$ are counterbalanced by one coordination complex cation $[Co(H_2O)_6]^{2+}$ and one alkali metal aqua cluster cation $\{Na_4(H_2O)_{14}\}^{4+}$. In the crystal structure, the sodium-aqua cluster cation $\{Na_4(H_2O)_{14}\}^{4+}$ is actually combination of $\{Na_{3.5}(H_2O)_{12}\}^{3.5+}$ and $\{Na(H_2O)_2\}^{0.5+}$, whereby both cationic species are coordinated to the decavanadate cluster anion by coordinate covalent bonds. Five sodium atoms (two Na3, full occupancy + two Na2, half occupancy + one Na1, half occupancy) form the $\{Na_{3.5}(H_2O)_{12}\}^{3.5+}$ cluster cation, coordinating to the decavanadate anion through Na1 cation and the rest sodium atom Na1 (from $\{Na(H_2O)_2\}^{0.5+}$ cationic species) coordinates to the same $\{V_{10}\}$ cluster from opposite side of the cluster anion. All sodium ions are octahedrally coordinated in the crystal structure. The coordination of $\{Na_4(H_2O)_{14}\}^{4+}$ cation to the $\{V_{10}\}$ cluster anion is shown in **Figure 2** (left). We believe that, the pH 9 of the concerned synthesis mixture is important in forming such $[Na_4(H_2O)_{14}]^{4+}$ cluster.

In the relevant crystal structure, this sodium aqua cluster cation self assembles to an infinite one-dimensional sodium water chain. These chains are laterally linked by $\{V_{10}O_{28}\}^{6-}$ cluster anions through Na1 ion resulting in a two-dimensional pure inorganic coordination polymer as shown in **Figure 2** (right). These two-dimensional sheets are stacked along crystallographic *a* axis as shown from the molecular packing diagram (**Figure 3**). The O–H···O hydrogen bonding situation in the crystal structure of $[Co(H_2O)_6][\{Na_4(H_2O)_{14}\}\{V_{10}O_{28}\}]\cdot 4H_2O$ (**1**) has been described in **Supplementary Figure 1** (Supporting Information). The relevant crystallographic data is available in **Table S1** (Supporting Information). **Tables S2, S3** (Supporting Information) have described bond distances along with bond angles and hydrogen bonding parameters respectively.

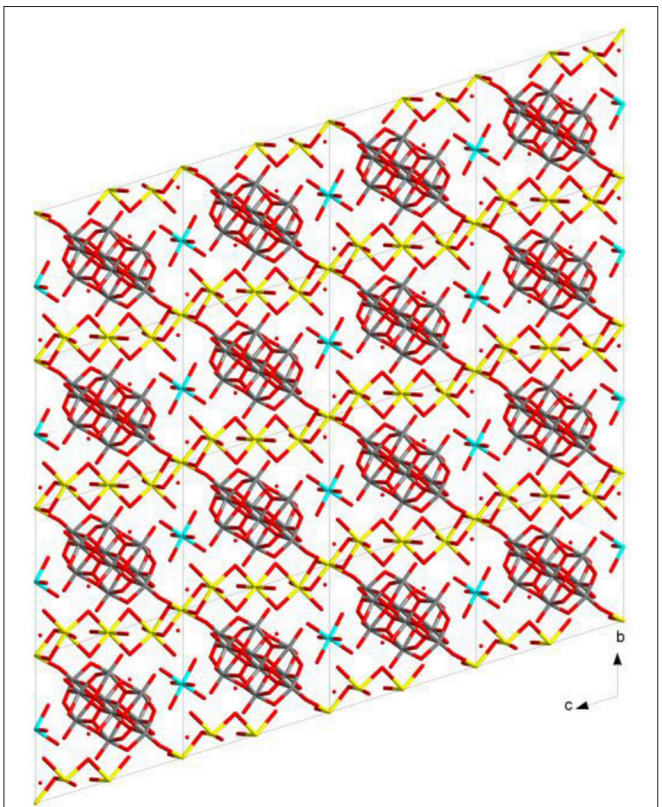

FIGURE 3 | Molecular packing diagram in the crystal structure of compound **1**.

Compound $[Zn(H_2O)_6][Na_3(H_2O)_{14}][HV_{10}O_{28}]\cdot 4H_2O$ (2)

The asymmetric unit in the crystal structure of compound **2** consists of two one-half decavanadate clusters, one tri-sodium aqua-complex $[Na_3(H_2O)_{14}]^{3+}$, one zinc hexa-aqua complex $[Zn(H_2O)_6]^{2+}$ and four solvent water molecules as shown in **Figure 4**. Thus the full molecule can be formulated as $[Zn(H_2O)_6][Na_3(H_2O)_{14}][HV_{10}O_{28}]\cdot 4H_2O$ (**2**), in which decavanadate cluster is singly protonated, and the rest of the charge (−5) is counter-balanced by $[Zn(H_2O)_6]^{2+}$ and $[Na_3(H_2O)_{14}]^{3+}$ cations. In the crystal structure, along with five lattice water molecules, fourteen water molecules are found to be coordinated with three sodium cations, resulting in the formation of $[Na_3(H_2O)_{14}]^{3+}$ cluster cation, in which the coordination of each sodium can be described by an octahedral arrangement of water molecules. The formation of this sodium-aqua cluster can be described by two terminal sodium ions (Na2 and Na3) and one middle sodium ion (Na1) as shown in **Figure 4** (top right).

The middle sodium ion (Na1) is coordinated to four μ_2-type bridging water molecules (O44, O47, O42, and O52) and two terminal water molecules (O46 and O50). Each of the terminal sodium ions is coordinated to two μ_2-type bridging water molecules and four terminal water molecules as shown in **Figure 4**. Hydrogen atoms could not be located for all the water molecules in the concerned crystal. By taking O···O separation in the range of 2.779 Å to 3.211 Å, supramolecular chemistry of compound **2** is described. A supramolecular $(H_2O)_9$ cluster is found to be formed by zinc- and sodium-coordinated water molecules and solvent water molecules. These $(H_2O)_9$ clusters are further linked by $(H_2O)_3$ cluster (shown

in blue dotted line) resulting in the formation of a chain-like arrangement as shown in **Figure 5**. The supramolecular O···O interactions between decavanadate cluster anions, the water chain and a (lattice) water dimer (O35···O35) lead to the generation of a supramolecular network as shown in **Figure 6**. This situation (**Figure 6**) can be depicted as inclusion of POV clusters in the water chain-network. In other words, it can be described that decavanadate cluster is stabilized in the pool of water.

$[HMTAH]_2[\{Zn(H_2O)_4\}_2\{V_{10}O_{28}\}]\cdot 2H_2O$ (3)

Compound **3**, that has been synthesized starting from sodium metavanadate, zinc nitrate and hexamine at pH 3.0 in a simple wet synthesis, crystallizes in monoclinic system with space group of $P2_1/c$. The concerned asymmetric unit consists of half of the decavanadate anion, one HMTAH cation and one zinc aqua complex cation (**Figure 7**). Thus it has been formulated as $[HMTAH]_2[\{Zn(H_2O)_4\}_2\{V_{10}O_{28}\}]\cdot 2H_2O$ (**3**). In the crystal structure, decavanadate moiety is functionalized by a Zn(II)-aqua complex, in which Zn1 is coordinated to two terminal oxo groups (O7 and O8) of both sides of decavanadate anion as shown in **Figure 7**. Thus the coordination number of zinc in polyoxovanadate (POV) supported Zn(II)-tetra-aqua coordination complex is six (two terminal oxygen and four water molecules). Two such POV supported Zn(II) coordination complexes form a $\{Zn_2\}$ dimer through two $\{\mu_2\text{-}H_2O\}$ type water bridges. Inter-dimer-decavanadate cluster coordination results in the formation of a 2-dimensional coordination polymer as shown **Figure 8**. Hydrogen bonding environment around $HMATAH^+$ moiety due to C–H···O interactions in the crystal structure of compound **3** is shown in **Supplementary Figure 2**. Hydrogen bond distances and angles are presented in **Table S4**.

Compound $[\{Co(3\text{-}amp)(H_2O)_5\}_2\{3\text{-}ampH\}_2][V_{10}O_{28}]\cdot 6H_2O$ (4)

A discrete inorganic-organic hybrid material $[Co(3\text{-}amp)(H_2O)_5]_2[3\text{-}ampH]_2\{V_{10}O_{28}\}\cdot 6H_2O$ (**4**) containing a

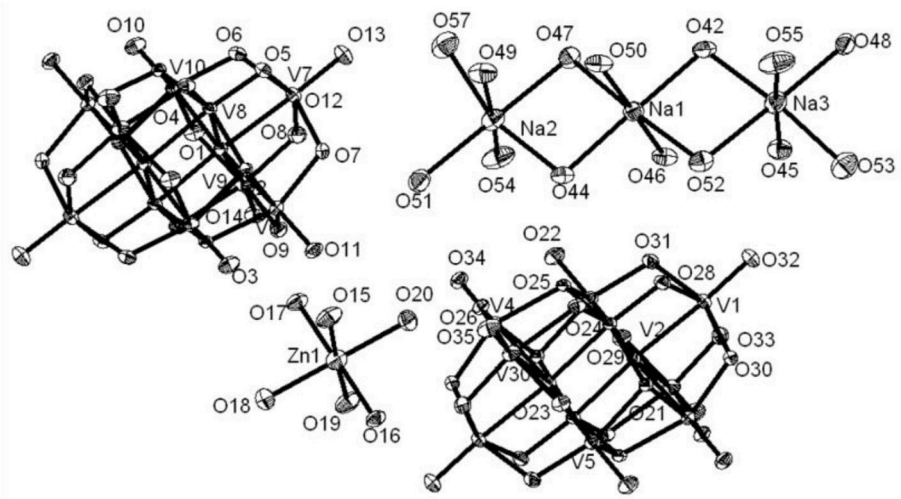

FIGURE 4 | Thermal ellipsoidal diagram of asymmetric part of compound $[Zn(H_2O)_6][Na_3(H_2O)_{14}][HV_{10}O_{28}]\cdot 4H_2O$ (**2**) with 30% probability (hydrogen atoms and solvent water molecules are omitted for clarity).

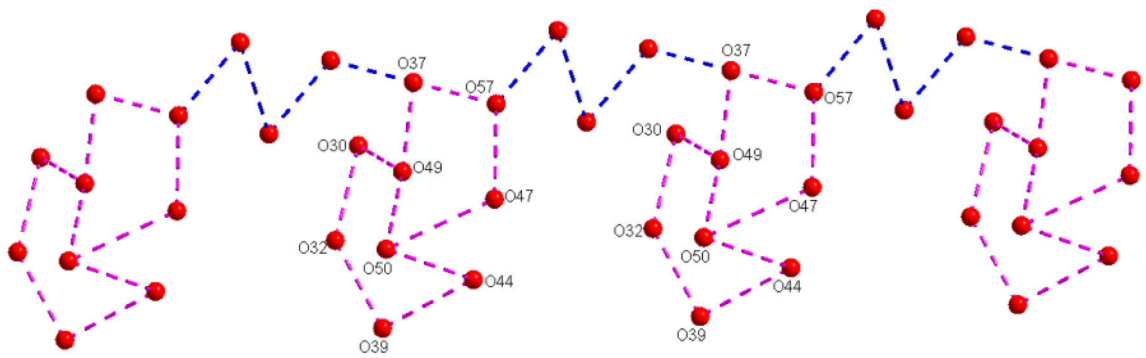

FIGURE 5 | A chainlike water structure, built from water cluster due to O–H···O interactions among the lattice water and zinc and sodium coordinated water molecules in the crystal structure of compound $[Zn(H_2O)_6][Na_3(H_2O)_{14}][HV_{10}O_{28}]\cdot 4H_2O$ (**2**).

cobalt complex, a decavanadate cluster anion, aminopyridinium cation and lattice water molecules, has been isolated with 3-aminopyridine in an aqueous medium in an one pot synthesis. Crystal system is confined with triclinic *P*-1 space group. The relevant asymmetric unit, as shown in **Figure 9**, reveals the presence of half of the decavanadate anionic cluster, one molecule of protonated 3-aminopyridine $[3\text{-ampH}]^{+}$ and a cobalt coordination complex $\{Co(3\text{-amp})(H_2O)_5\}^{2+}$. Apart from columbic interaction between cation and anionic species, non-covalent interactions are also responsible for stability of the compound **4**. In the crystal structure, a three-dimensional framework has been built due to C–H···O hydrogen bonding interactions between the cationic part and decavanadate anionic cluster as shown in **Figure 10**. Hydrogen bonding situation around the 3-aminopryridines (coordinated as well as cation) and water molecule, is shown in **Supplementary Figure 3** and their hydrogen bonding distances and angles are shown in **Table S5** including pertinent symmetry operations. We found weak π-π interactions among the molecules of 3-aminopyridine (see **Supplementary Figure 4**).

Compound $[4\text{-ampH}]_{10}[\{Na(H_2O)_6\}\{HV_{10}O_{28}\}][V_{10}O_{28}]\cdot 15H_2O$ (5)

Asymmetric unit of the crystal structure of compound **5** reveals that two independent halves of decavanadate anionic cluster $[V_{10}O_{28}]^{6-}$ are assembled with the five cation molecules of 4-ampH^{+} and a $Na(H_2O)_3$ moiety with sodium in special position.

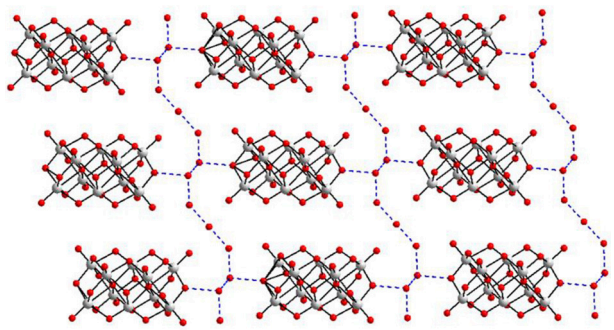

FIGURE 6 | A hydrogen-bonded supramolecular array consisting of decavanadate cluster anion and water molecules including lattice waters and metal coordinated water molecules.

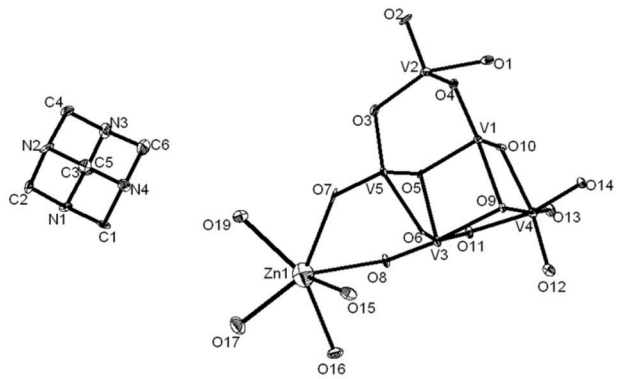

FIGURE 7 | Thermal ellipsoidal diagram of asymmetric part of compound $[HMTAH]_2[\{Zn(H_2O)_4\}_2\{V_{10}O_{28}\}]\cdot 2H_2O$ (**3**).

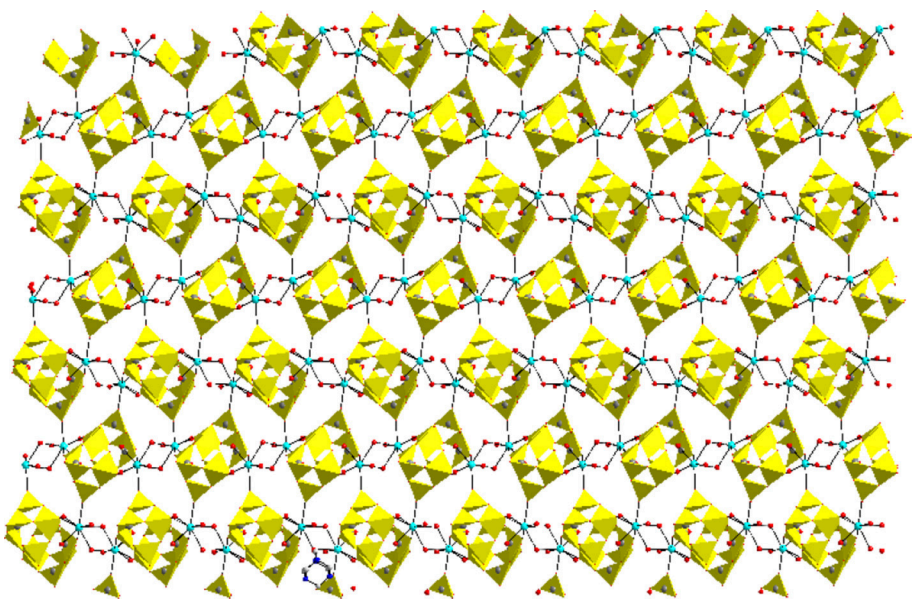

FIGURE 8 | Two-dimensional coordination polymer, formed in the crystal structure of $[HMTAH]_2[\{Zn(H_2O)_4\}_2\{V_{10}O_{28}\}]\cdot 2H_2O$ (**3**). Color codes: V–O polyhedra, yellow; Zn, Cyan; O, red.

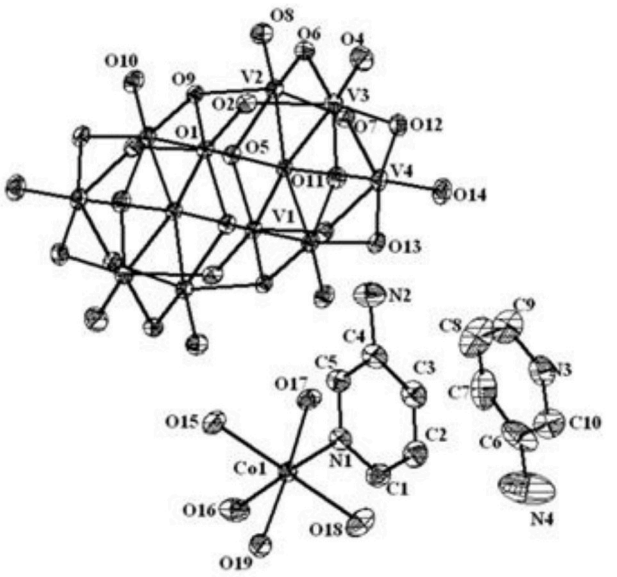

FIGURE 9 | Thermal ellipsoidal diagram of $[\{Co(3\text{-amp})(H_2O)_5\}_2\{3\text{-ampH}\}_2][V_{10}O_{28}]\cdot 6H_2O$ (**4**) with 30% probability (hydrogen atoms are omitted for clarity).

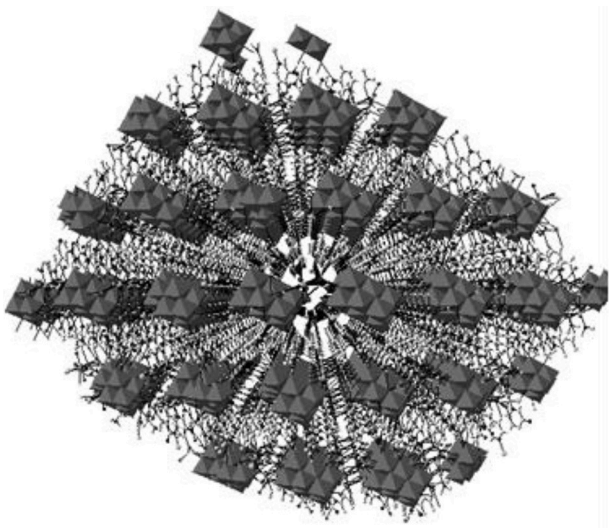

FIGURE 10 | A 3-dimensional framework (a perspective view), generated due to C–H···O hydrogen bonding interactions between cation and decavanadate anion in the crystal of compound $[\{Co(3\text{-amp})(H_2O)_5\}_2\{3\text{-ampH}\}_2][V_{10}O_{28}]\cdot 6H_2O$ (**4**).

ORTEP diagram of the $[4\text{-ampH}]_{10}[\{Na(H_2O)_6\}\ \{HV_{10}O_{28}\}][V_{10}O_{28}]\cdot 15H_2O$ (**5**) is shown in the **Figure 11**. We have found ten lattice water molecules in the crystal structure of **5** and a cyclic water pentamer is generated due of the O–H···O hydrogen bonding interactions among the water molecules: O28, O29, O30, O33, and O36 as shown in **Figure 12**, left. Two such water pentamers are connected with a central sodium hexa-aqua complex *via* Na–O–H···O (pentamer) interactions resulting in the generation of a dumbbell-shaped-supramolecular architecture as presented in **Figure 12**, right. The relevant crystallographic data is provided in **Table 2**. And C–H···O and O–H···O hydrogen bonding interactions around {N1N2}, {N3N4}, {N5N6}, {N7N8}, {N9N10}, and water moieties in the crystal structure of **5** are shown in **Supplementary Figure 5** and pertinent hydrogen bond distances and angles are listed in the **Table S6** including symmetry operations.

Compound $[\{4\text{-ampH}\}_6\{Co(H_2O)_6\}_3][V_{10}O_{28}]_2\cdot 14H_2O$ (6)

The asymmetric unit of compound **6** (**Figure 13**) consists of two independent haves of decavanadate $\{V_{10}O_{28}\}^{6-}$ cluster anion, 1.5 molecules of $[Co(H_2O)_6]^{2+}$, three protonated 4-aminopyridine and seven solvent water molecules. Accordingly, this is formulated as $[\{4\text{-ampH}\}_6\{Co(H_2O)_6\}_3][V_{10}O_{28}]_2\cdot 14H_2O$ (**6**). In the crystal structure, coordinated water molecules and lattice water molecules are non-covalently interacted through hydrogen bonding, generating a water tetramer (O30, O39, O35, O31) with O···H distances of 2.01 Å, 1.842 Å, and 2.077 Å, respectively (**Figure 14**) and each end oxygen atoms of the water tetramer, i.e., O30 and O31, is linked to cobalt center of the cobalt-hexa-aqua complex. Hydrogen bonding situation around {N1N2}, {N3N4}, {N5N6}, {N7N8}, {N9N10}, {Co} and water in the crystal structure of **6** is shown in **Supplementary Figure 6**, which is explained based on C–H···O, O–H···O, and N–H···O interactions. The relevant hydrogen bond distances and angles are listed in the **Table S7** in the section of **Supplementary Material**.

Compound $[\{4\text{-ampH}\}_{10}\{Zn(H_2O)_6\}][V_{10}O_{28}]_2\cdot 10H_2O$ (7)

The crystal structure of $[\{4\text{-ampH}\}_{10}\{Zn(H_2O)_6\}][V_{10}O_{28}]_2\cdot 10H_2O$ (**7**) has been characterized with the monoclinic, $P2_1/c$ space group. It consists of two clusters of decavanadate anion $\{V_{10}O_{28}\}^{6-}$, ten molecules of protonated 4-aminopyridine and one unit of zinc(II)-hexa-aqua complex $[Zn(H_2O)_6]^{2+}$. In addition, ten lattice water molecules are crystallized in the crystal structure of compound **7**. Thermal ellipsoidal diagram of compound **7** is presented in **Figure 15**. In the crystal structure, lattice water molecules (O36, O37, O40, O38), and coordinated water molecule (O16) are non-covalently interacted due to O–H···O hydrogen bonding interactions resulting in the generation of a cyclic water pentamer, that has been represented in **Figure 16**, left. In this supramolecular water pentamer, since the O16 water is the Zn(II)-coordinated water molecule and it is equivalent to another O16 by a symmetry operation coordinated to same Zn(II), it is possible to have two water pentamers connected by a central Zn(II) ion resulting in dumbbell-like construction as shown in **Figure 16**, right (O···H distances lie between 2.007 Å and 2.158 Å). Hydrogen bonding situations around {N1N2}, {N3N4}, {N5N6}, {N7N8}, {N9N10}, {Zn} and water due to C–H···O, N–H···O and O–H···O interactions in the crystal structure of **7** are shown in **Supplementary Figure 7** and relevant hydrogen bond

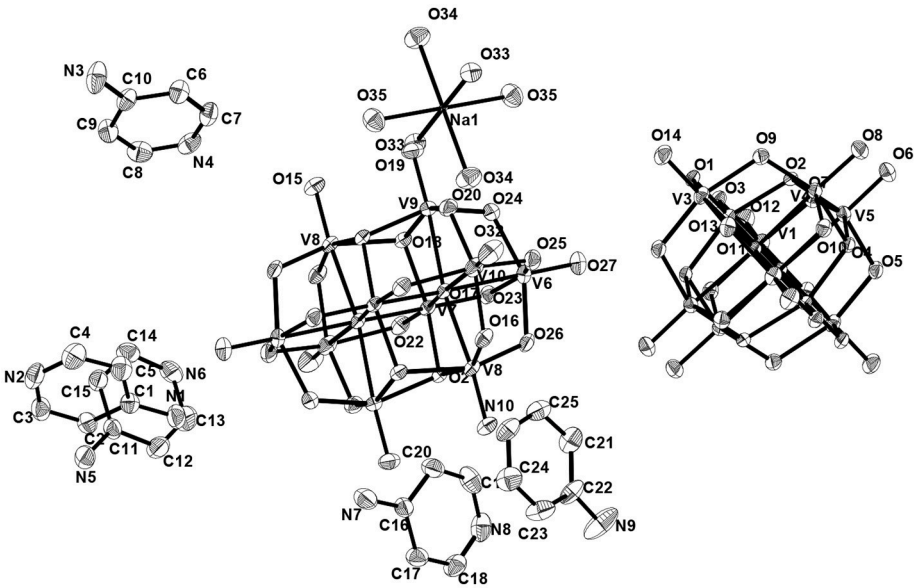

FIGURE 11 | Thermal ellipsoidal Thermal Ellipsoidal diagram of $[4\text{-ampH}]_{10}[\{Na(H_2O)_6\}\ \{HV_{10}O_{28}\}]\ [V_{10}O_{28}]\cdot 15H_2O$ (**5**) with 30% probability (hydrogen atoms are omitted for clarity).

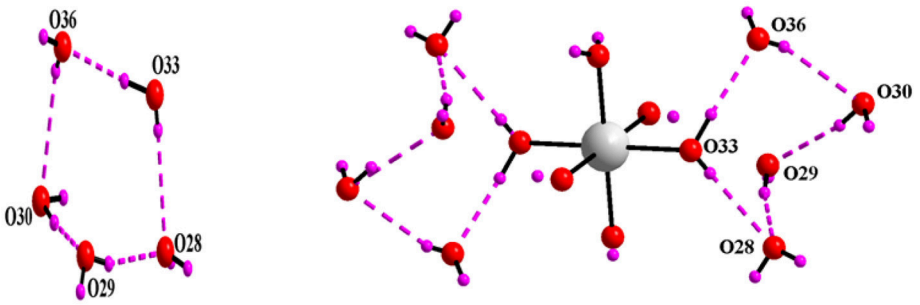

FIGURE 12 | Left: cyclic water pentamer is generated due to O–H···O interactions in $[4\text{-ampH}]_{10}[\{Na(H_2O)_6\}\ \{HV_{10}O_{28}\}]\ [V_{10}O_{28}]\cdot 15H_2O$ (**5**); **right:** dumbbell shape diagram due to O–H···O interaction in 6 involving $\{Na(H_2O)_6\}$ coordination complex. Color codes: O, red; Na, grey; H, purple.

distances and angles are given in **Table S8** with symmetry codes.

Understanding Decavanadate-Based Mineralogy

Until now, more than 12 decavanadate based minerals have been known (**Table 3**) and interestingly, many of them have been characterized by crystallography. Out of seven described compounds in this work, two compounds $[Co(H_2O)_6][\{Na_4(H_2O)_{14}\}\{V_{10}O_{28}\}]\cdot 4H_2O$ (**1**) and $[Zn(H_2O)_6]\ [Na_3(H_2O)_{14}]\ [HV_{10}O_{28}]\cdot 4H_2O$ (**2**) have direct relevance to the decavanadate-based mineral. For example, the mineral kokinosite, $Na_2Ca_2(V_{10}O_{28})\bullet 24H_2O$ (Kampf et al., 2014) and compound $[Co(H_2O)_6][\{Na_4(H_2O)_{14}\}\{V_{10}O_{28}\}]\cdot 4H_2O$ (**1**) (the formula of which can also be written as $Na_4Co\ (V_{10}O_{28})\bullet 24H_2O$) can be discussed in the context of the microenvironment of the isopolyanion $[V_{10}O_{28}]^{6-}$ in this synthesized compound **1** and in kokinosite. Both compound **1** and the kokinosite mineral have similar / comparable crystal cell parameters and crystallize in the same space group. In the crystal structure of compound **1**, we have found the abundance of $\{Na_4(H_2O)_{14}\}^{4+}$ liner-shaped water-bridged cluster (per formula unit), which is coordinated to the decavanadate cluster anion through terminal oxygen of the polyanion. In other words, in the synthesized compound **1**, decavanadate supported sodium-water cluster $\{Na_4(H_2O)_{14}\}^{4+}$ exists (**Figure 2**). In the relevant crystal structure, the interlinking of these clusters results in the infinite sodium-water chain. These sodium-water chains are laterally linked by the decavanadate anions to form a two-dimensional coordination polymeric structure; $[Co(H_2O)_6]^{2+}$ remains as an isolated discrete coordination complex cation located in the void space (**Figure 3**) to counterbalance the negative charges

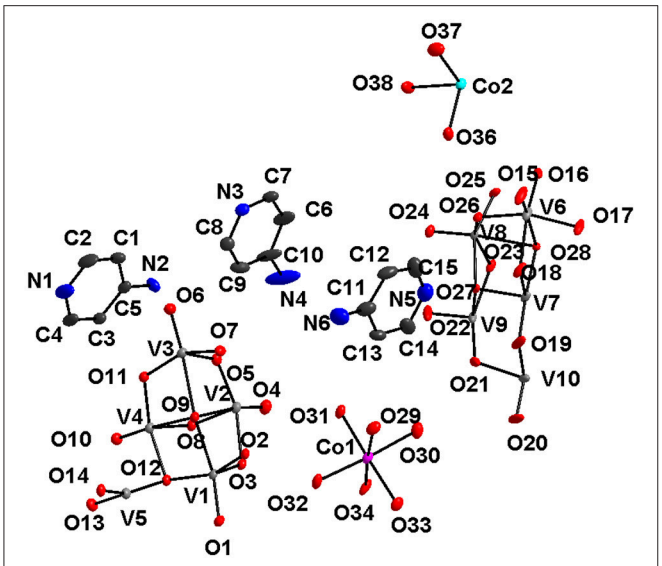

FIGURE 13 | Thermal ellipsoidal plot of the asymmetric unit of compound $[\{4\text{-ampH}\}_6\{Co(H2O)_6\}_3][V10O28]_2\cdot 14H_2O$ (6) (hydrogen atoms and solvent water molecules are omitted for clarity). Color codes: O, red; V, medium grey; C, dark grey; Co, cyan.

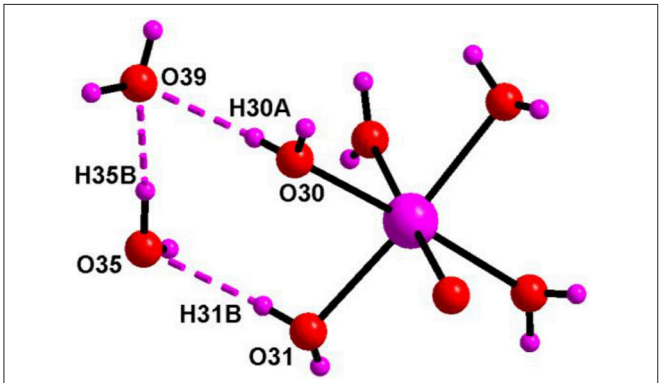

FIGURE 14 | Supramolecular water tetramer, generated due to O–H···O interactions in the crystal of $[\{4\text{-ampH}\}_6\{Co(H_2O)_6\}_3][V_{10}O_{28}]_2\cdot 14H_2O$ (**6**) involving the cobalt complex. Color codes: O, red; H and Co, purple.

of the decavanadate anion. In the language of decavanadate mineral crystallography, these cations (e.g., sodium and cobalt ions in compound **1**) are called interstitial units (Hughes et al., 2002, 2005, 2008; Colombo et al., 2011; Kampf et al., 2011b, 2013b, 2014). For example, in the crystal structure of the kokinosite mineral (Kampf et al., 2014), the interstitial unit has a composition of $(Na_2Ca_2\bullet 24H_2O)^{6+}$ and the decavanadate anion $(V_{10}O_{28})^{6-}$ forms the structural unit of the mineral. In the relevant crystal structure (kokinosite), the decavandate cluster anions (structural units) are linked by $Na(H_2O)_6$ octahedra (interstitial units) and $Ca(H_2O)_8$ polyhedra (interstitial units) that themselves link into infinite chains by edge and corner sharing. So in this case, $Ca(H_2O)_8$ is part of the infinite chain (unlike $Co(H_2O)_6$ in compound **1**, that remains as a isolated complex cation). Overall, both structures are comparable.

Compound $[Zn(H_2O)_6][Na_3(H_2O)_{14}][HV_{10}O_{28}]\cdot 4H_2O$ (**2**), synthesized and characterized in this work, is formulated with a mono-protonated decavanadate cluster anion $[HV_{10}O_{28}]^{5-}$. In 2011, Kampf et al. reported diprotonated decavanadate based mineral, gunterite $Na_4(H_2V_{10}O_{28})\bullet 22H_2O$ (Kampf et al., 2011b). In both the crystal structures, the proton on the decavanadate anion could not be located, but formulated from elemental analyses and crystallographic investigation on the cationic part. In the crystal structure of compound **2**, a sodium trimer-water cluster $[Na_3(H_2O)_{14}]^{3+}$ per formula unit is characterized, which unlike compound 1 is not coordinated to decavanadate anion. But in the case of the gunterite mineral, the sodium water cluster is coordinated to the polyanion (Kampf et al., 2011b). In the crystal structure of synthesized compound **2**, the $[Zn(H_2O)_6]^{2+}$ moiety remains as an isolated discrete coordination complex cation, counter balancing the residual charge of the decavanadate anion. In most of these mineral structures, solvent waters are found disordered; on the other hand, in most of the synthesized compounds (present work), lattice waters are characterized as forming supramolecular water clusters. So far, no decavanadate based minerals are found, in which the interstitial cation is a transition metal-aqua complex cation, as synthesized in the present work. The present synthesis work predicts that the formation of such transition metal cation associated decavanadate minerals is possible and we expect that transition metal decavanadate minerals will be discovered in future that may feature the presence of discrete hexa-aqua transition metal coordination complex as an interstitial cation, as found in the present model study.

CONCLUSIONS

We have described the synthesis and characterization of seven decavanadate containing compounds $[Co(H_2O)_6][\{Na_4(H_2O)_{14}\}\{V_{10}O_{28}\}]\cdot 4H_2O$ (**1**), $[Zn(H_2O)_6][Na_3(H_2O)_{14}][HV_{10}O_{28}]\cdot 4H_2O$ (**2**), $[HMTAH]_2[\{Zn(H_2O)_4\}_2\{V_{10}O_{28}\}]\cdot 2H_2O$ (**3**), $[\{Co(3\text{-amp})(H_2O)_5\}_2\{3\text{-ampH}\}_2][V_{10}O_{28}]\cdot 6H_2O$ (**4**), $[4\text{-ampH}]_{10}[\{Na(H_2O)_6\}\{HV_{10}O_{28}\}][V_{10}O_{28}]\cdot 15H_2O$ (**5**), $[\{4\text{-ampH}\}_6\{Co(H_2O)_6\}_3][V_{10}O_{28}]_2\cdot 14H_2O$ (**6**), $[\{4\text{-ampH}\}_{10}\{Zn(H_2O)_6\}][V_{10}O_{28}]_2\cdot 10H_2O$ (**7**). In this report, we have described detailed supramolecular chemistry of **1**−7. In some of their crystal structures, non-covalent interactions among the lattice water molecules and metal coordinated water molecules lead to the formation of supramolecular water clusters. Thus the microenvironment of the decavanadate cluster anion in diverse cation matrices includes the formation of ordered water structures. We have also observed that, in these decavanadate based systems, the transition metal aqua complexes like to remain as discrete coordination complex cation, whereas the alkali metal aqua complexes like to aggregate to dimer, trimer, tetramer, infinite chain etc. These alkali metal water aggregations mimic the interstitial units of natural minerals of decavanadates. We have discussed the supramolecular chemistry of the synthesized systems comparing the microenvironment of decavanadate cluster anion, found in natural minerals.

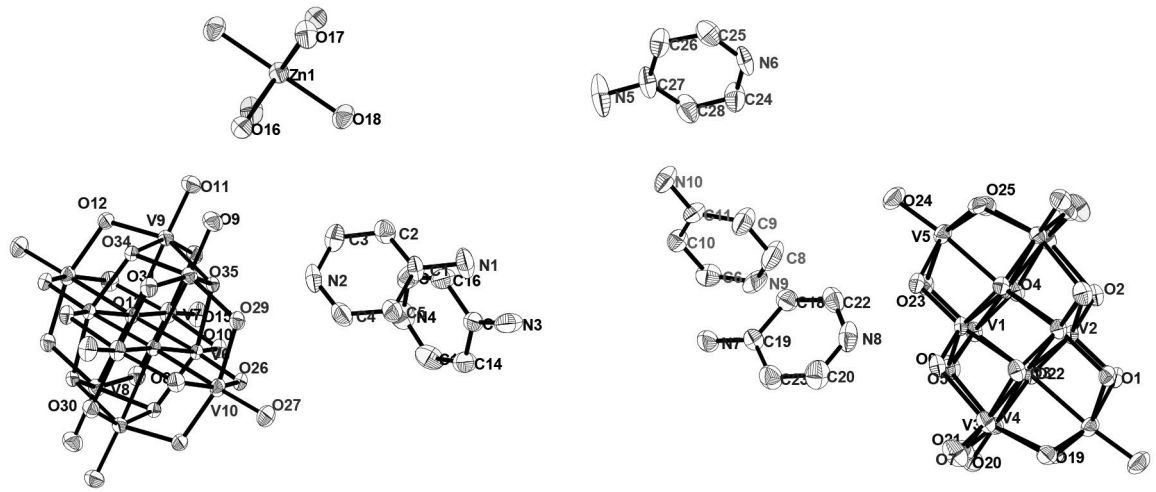

FIGURE 15 | ORTEP diagram in the crystal structure of compound $[\{4\text{-ampH}\}_{10}\{Zn(H_2O)_6\}][V_{10}O_{28}]_2 \cdot 10H_2O$ (**7**) with 30% probability (hydrogen atoms and solvent water molecules are omitted for clarity).

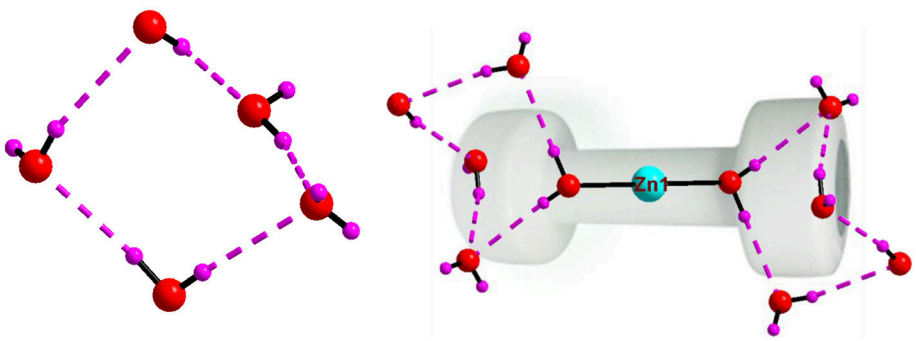

FIGURE 16 | Left: cyclic water pentamer, generated due to O–H···O interactions in compound $[\{4\text{-ampH}\}_{10}\{Zn(H_2O)_6\}][V_{10}O_{28}]_2 \cdot 10H_2O$ (**7**); **right:** dumbbell shape diagram due to O–H···O interactions in **7** involving $\{Zn(H_2O)_6\}$ coordination complex and water pentamers. Color codes: O, red; Zn, cyan; H, purple.

AUTHOR CONTRIBUTIONS

SA was Ph.D. student and SD is his Ph.D. supervisor. SA synthesized and characterized the compounds, described in this manuscript under the supervision of SD. Both SA and SD analyzed the data together. This manuscript has been written by SD mainly, but it was shown to SA. SA has agreed with the content of the manuscript.

ACKNOWLEDGMENTS

We thank, SERB, Department of Science and Technology, Government of India, for financial support (Project No. EMR/2017/002971). We also thank Center for Nano Technology, University of Hyderabad. The National X-ray Diffractometer facility at the University of Hyderabad by the Department of Science and Technology, Government of India, is gratefully acknowledged. SA thank CSIR, Government of India for his fellowship. We acknowledge DST-PURSE, UPE-II, and UGC-CAS.

SUPPLEMENTARY MATERIAL

The Supplementary Material for this article can be found online at: https://www.frontiersin.org/articles/10.3389/fchem.2018.00469/full#supplementary-material

REFERENCES

Al-Qatati, A., Fontes, F. L., Barisas, B. G., Zhang, D., Roessa, D. A., and Debbie, C., et al. (2013). Raft localization of Type I Fcε receptor and degranulation of RBL-2H3 cells exposed to decavanadate, a structural model for V_2O_5. *Dalton Trans.* 42, 11912–11920. doi: 10.1039/c3dt50398d

Amini, M., Nikkhoo, M., Tekantappeh, S. B., Farnia, S. M. F., Mahmoudi, G., and Büyükgüngör, O. (2017). Synthesis, characterization and catalytic

properties of a copper complex containing decavanadate nanocluster, $Na_2[Cu(H_2O)_6]_2\{V_{10}O_{28}\}\cdot 4H_2O$. *Inorg. Chem. Commun.* 77, 72–76. doi: 10.1016/j.inoche.2017.02.001

Arumuganathan, T., and Das, S. K. (2009). Discrete polyoxovanadate cluster into an organic free metal-oxide-based material: syntheses, crystal structures, and magnetic properties of a new series of lanthanide linked-POV compounds [{Ln(H2O)6}2As8V14O42(SO3)] · 8H2O (Ln = La3+, Sm3+, and Ce3+). *Inorg. Chem.* 48, 496–507. doi: 10.1021/ic8002383

Aureliano, M., and Crans, D. C. (2009). Decavanadate (V10O286-) and oxovanadates: oxometalates with many biological activities. *J. Inorg. Biochem.* 103, 536–546. doi: 10.1016/j.jinorgbio.2008.11.010

Aureliano, M., Fraqueza, G., and Ohlin, C. A. (2013). Ion pumps as biological targets for decavanadate. *Dalton Trans.* 42, 11770–11777. doi: 10.1039/c3dt50462j

Chatkon, A., Barres, A., Samart, N., Boyle, S. E., Haller, K. J., and Crans, D. C. (2014). Guanylurea metformium double salt of decavanadate, $(HGU^+)_4(HMet^+)_2(V_{10}O_{28}^{6-})\cdot 2H_2O$. *Inorg. Chem. Acta.* 420, 85–91. doi: 10.1016/j.ica.2013.12.031

Chatkon, A., Chatterjee, P. B., Sedgwick, M. A., Haller, K. J., and Crans, D. C. (2013). Counterion affects interaction with interfaces: the antidiabetic drugs metformin and decavanadate. *Eur. J. Inorg. Chem.* 2013, 1859–1868. doi: 10.1002/ejic.201201345

Chen, J.-J., Ye, J.-C., Zhang, X.-G., Symes, M. D., Fan, S.-C., Long, D.-L., et al. (2018). Design and performance of rechargeable sodium ion batteries, and symmetrical Li-ion batteries with supercapacitor-like power density based upon polyoxovanadates. *Adv. Energy Mater.* 8:1701021. doi: 10.1002/aenm.201701021

Chen, L., Jiang, F., Lin, Z., Zhou, Y., Chengyang Yue, C., and Hong, M. (2005). Basket tetradecavanadate cluster with blue luminescence. *J. Am. Chem. Soc.* 127, 8588–8589. doi: 10.1021/ja0422209

Colombo, F., Baggio, R., and Kampf, A. R. (2011). The crystal structure of elusive heumulite. *Can. Mineral.* 49, 849–864. doi: 10.3749/canmin.49.3.849

Conte, V., and Floris, B. (2010). Vanadium catalyzed oxidation with hydrogen peroxide. *Inorg. Chim. Acta* 363, 1935–1946. doi: 10.1016/j.ica.2009.06.056

Crans, D. C., Mahroof-Tahir, M., Anderson, O. P., and Miller, M. M. (1994). X-ray structure of $(NH_4)_6(Gly\text{-}Gly)_2V_{10}O_{28}\cdot 4H_20$ model studies for polyoxometalate—protein interactions. *Inorg. Chem.* 33, 5586–5590.

Crans, D. C., Peters, B. J., Wu, X., and McLauchlan, C. C. (2017). Does anion-cation organization in Na+-containing X-ray crystal structures relate to solution interactions in inhomogeneous nanoscale environments: Sodium-decavanadate in solid state materials, minerals, and microemulsions. *Coordination Chem. Rev.* 344, 115–130. doi: 10.1016/j.ccr.2017.03.016

Crans, D. C., Smee, J. J., Gaidamauskas, E., and Yang, L. (2004). The chemistry and biochemistry of vanadium and the biological activities exerted by vanadium compounds. *Chem. Rev.* 104, 849–902. doi: 10.1021/cr020607t

da Silva, J. L. F., da Piedada, M. F. M., and Duarta, M. T. (2003). Decavanadates: a building-block for supramolecular assemblies. *Inorg. Chim. Acta* 356, 222–242. doi:10.1016/S0020-1693(03)00385-2

Derat, E., Kumar, D., Neumann, R., and Shaik, S. (2006). Catalysts for monooxygenations made from polyoxometalate: an iron(V)-oxo derivative of the Lindqvist anion. *Inorg. Chem.* 45, 8655–8663. doi: 10.1021/ic0610435

Gao, F., and Hua, R. (2006). An efficient polyoxovanadate-catalyzed oxidative mineralization of phenols with 30% aqueous H_2O_2. *Catalysis Commun.* 7, 391–393. doi: 10.1016/j.catcom.2005.12.013

Guo, Y., Wang, Y., Hu, C., Wang, Y., Wang, E., Zhou, Y., et al. (2000). Microporous polyoxometalates POMs/SiO2: synthesis and photocatalytic degradation of aqueous organocholorine pesticides. *Chem. Mater.* 12, 3501–3508. doi: 10.1021/cm000074

Hill, C. L. (2007). Progress and challenges in polyoxometalate-based catalysis and catalytic materials chemistry. *J. Mol. Catalysis A Chem.* 262, 2–6. doi: 10.1016/j.molcata.2006.08.042

Huang, X., Li, J., Shen, G., Xin, N., Lin, Z., Chi, Y., et al. (2018). Three Pd-decavanadates with a controllable molar ratio of Pd to decavanadate and their heterogeneous aerobic oxidation of benzylic C–H bonds. *Dalton Trans.* 47, 726–733. doi: 10.1039/C7DT03898D

Hughes, J. M., Schindler, M., and Francies, C. A. (2005). The C2/m disordered structure of pascoite, $Ca_3(V_{10}O_{28})\bullet 17H_2O$. *Can. Mineral.* 43, 1379–1386. doi: 10.2113/gscanmin.43.4.1379

Hughes, J. M., Schindler, M., Rakovan, J., and Cureton, F. E. (2002). The crystal structure of hummerite. $KMg(V_5O_{14})\bullet 8H_2O$: bonding between the $[V_{10}O_{28}]^{6-}$ structural unit and the $\{K_2Mg_2(H_2O)_{16}\}^{6+}$ interstitial complex. *Can. Mineral.* 40, 1429–1435. doi: 10.2113/gscanmin.40.5.1429

Hughes, J. M., Wise, W. S., Gunter, M. E., Morton, J. P., and Rakovan, J. (2008). A new decavamadate mineral species from the vanadium Queen Mine, La Sal district, Utah: description, atomic arrangement, and relationship to the pascoite group of minerals. *Can. Mineral.* 46, 1365–1372. doi: 10.3749/canmin.46.5.1365

Kampf, A. R., Hughes, J. M., Marty, and Brown, F. H. (2013a). Nashite, $Na_3Ca_2([V_9^{5+}V_1^{4+}]O_{28})\bullet 24H_2O$, a new mineral species from the Yellow Cat Mining District, Utah and the slick rock mining district, Colorado: crystal structure and descriptive mineralogy. *Can. Mineral.* 51, 27–37. doi: 10.3749/canmin.51.1.27

Kampf, A. R., Hughes, J. M., Marty, J., Gunter, M. E., and Nash, B. (2011a). Rakovanite, $Na_3\{H_3[V_{10}O_{28}]\}\bullet 15H_2O$, a new species of the pascoite family with a protonated decavanadate polyanion. *Can. Mineral.* 49, 889–898. doi: 10.3749/canmin.49.2.595

Kampf, A. R., Hughes, J. M., Marty, J., and Nash, B. (2011b). Gunterite, $Na_4(H_2O)_{16}(H_2V_{10}O_{28})\bullet 6H_2O$, a new mineral with a doubly-protonated decavanadate polyanion: crystal structure and descriptive mineralogy. *Can. Mineral.* 49, 1243–1251. doi: 10.3749/canmin.49.5.1243

Kampf, A. R., Hughes, J. M., Marty, J., and Nash, B. (2012). Postite, $Mg(H_2O)_6Al_2(OH)_2(H_2O)_8(V_{10}O_{28})\bullet 13H_2O$, a new mineral species from the La Sal mining district, Utah: crystal structure and descriptive mineralogy. *Can. Mineral.* 50, 45–53. doi: 10.3749/canmin.50.1.45

Kampf, A. R., Hughes, J. M., Marty, J., and Nash, B. (2013b). Wernerbaurite, $\{[Ca(H_2O)_7]_2(H_2O)_2(H_3O)_2\}\{V_{10}O_{28}\}$, and schindlerite, $\{[Na_2(H_2O)_{10}](H_3O)_4\}\{V_{10}O_{28}\}$, the first hydronium-bearing decavanadate minerals. *Can. Mineral.* 51, 297–312. doi: 10.3749/canmin.51.2.297

Kampf, A. R., Hughes, J. M., Nash, B., and Marty, J. (2014). Kokinosite, Na2Ca2(V10O28) •24H2O, a new decavanadate mineral species from the St. Jude Mine, Colorado: crystal structure and descriptive mineralogy. *Can Mineral.* 52, 15–25. doi: 10.3749/canmin.52.1.15

Kampf, A. R., and Steele, I. M. (2008). Magnesiopascoite, a new member of the pascoite group: description and crystal structure. *Can. Mineral.* 46, 679–686. doi: 10.3749/canmin.46.3.679

Khan, M. I., Yohannes, E., and Doedens, R. J. (2003). A novel series of materials composed of arrays of vanadium oxide container molecules, {V18O42(X)} (X) H2O, Cl-, Br-): synthesis and characterization of M2(H2N(CH2)2NH2)5][{M(H2N(CH2)2NH2)2}2V18O42(X)]·9H2O (M = Zn, Cd). *Inorg. Chem.* 42, 3125–3129. doi: 10.1021/ic025889u

Klemperer, W. G., Marquart, T. A., and Yaghi, O. M. (1992). New directions in polyvanadate chemistry: from cages and clusters to baskets, belts, bowls, and barrels. *Angew. Chem.* 31, 49–51. doi: 10.1002/anie.199200491

Koene, B. E., Taylor, N. J., and Nazar, L. F. (1999). An inorganic tire-tread lattice: hydrothermal synthesis of the layered vanadate [N(CH3)4]5V18O46 with a supercell structure. *Angew. Chem. Int. Ed.* 38, 2888–2891. doi: 10.1002/(SICI)1521-3773

Kulikov, V., and Meyer, G. (2013). A new strategy for the synthetic assembly of inorganic-organic silver(I)-polyoxometalate hybrid structures employing noncovalent interactions between theobromine ligands. *Cryst. Growth Des.* 13, 2916–2927. doi: 10.1021/cg400335y

Kwon, T., Tsigdinos, G. A., and Pinnavaia, T. J. (1988). Pillaring of layered double hydroxides (LDH's) by polyoxometalate anions. *J. Am. Chem. Soc.* 110, 3653–3654. doi: 10.1021/ja00219a048

Lechner, M., Güttel, R., and Streb, C. (2016). Challenges in polyoxometalate-mediated aerobic oxidation catalysis: catalyst development meets reactor design. *Dalton Trans.* 45, 16716–16726. doi: 10.1039/c6dt03051c

Liu, S., Tian, J., Wang, L., Zhang, Y., Luo, Y., Li, H., et al. (2012). Fast and sensitive colorimetric detection of H_2O_2 and glucose: a strategy based on polyoxometalate clusters. *ChemPlusChem* 77, 541–544. doi: 10.1002/cplu.201200051

Marques, M. P. M., Gianolio, D., Ramos, S., de Carvalho, L. A. E., and Aureliano, M. (2017). An EXAFS approach to the study of polyoxometalate–protein interactions: the case of decavanadate–Actin. *Inorg. Chem.* 56, 10893–10903. doi: 10.1021/acs.inorgchem.7b01018

Martín-Caballero, J., San José Wéry A., Reinoso, S., Artetxe, B., San Felices, L. E., Bakkali, B. et al. M. (2016). A robust open framework formed by decavanadate clusters and copper(II) complexes of macrocyclic polyamines: permanent microporosity and catalytic oxidation of cycloalkanes. *Inorg. Chem.* 55, 4970–4979. doi: 10.1021/acs.inorgchem.6b00505

Mestiri, I., Ayed, B., and Haddad, A. (2013). Two novel compounds built up of decavanadate clusters and transition-metal complexes: synthesis and structure. *J Clust. Sci*. 24, 85–96. doi: 10.1007/s10876-012-0517-4

Miiller, A., Krickerneyer, E., Penk, M., Walberg, H.-J., and Bogge, H. (1987). Spherical mixed-valence $[V_{15}O_{36}]^{5-}$, an example from an unusual cluster family. *Angew. Chem.* 26, 1045–1046. doi: 10.1002/anie.198710451

Miiller, A., Penk, M., Rohljing, R., Krickemeyer, E., and Döring, J. (1990). Topologically interesting cages for negative ions with extremely high "coordination number": an unusual property of V-0 clusters. *Angew. Chem. Int. Ed.* 29, 926–927. doi: 10.1002/anie.199009261

Mukhopadhyay, S., Debgupta, J., Singh, C., Kar, A., and Das, S. K. (2018). A Keggin polyoxometalate shows water oxidation activity at neutral pH: POM@ZIF-8, an efficient and robust electrocatalyst. *Angew. Chem. Int. Ed.* 57, 1918–1923. doi: 10.1002/anie.201711920

Müller, A., Sessoli, R., Krickemeyer, E., Bögge, H., Meyer, J., Gatteschi, D., et al. (1997). Polyoxovanadates: high-nuclearity spin clusters with interesting host-guest systems and different electron populations. Synthesis, spin organization, magnetochemistry, and spectroscopic studies. *Inorg. Chem.* 36, 5239–5250. doi: 10.1021/ic9703641

Naslhajian, H., Amini, M., Farnia, S. M. F., Sheykhi, A., Sahin, O., and Okan Zafer Yeşilel, O. Z. (2017). A new decavanadate polyoxovanadate nanocluster: synthesis, characterization and rapid adsorption of methylene blue. *J. Coord. Chem.* 70, 2940–2949. doi: 10.1080/00958972.2017.1383601

Omwoma, S., Gore, C. T., Ji, Y., Hu, C., and Song, Y.-F. (2015). Environmentally benign polyoxometalate materials. *Coordination Chem. Rev.* 286, 17–29. doi: 10.1016/j.ccr.2014.11.013

Pope, M. T., and Müller, A. (1991). Polyoxometalate chemistry: an old field with new dimensions in several disciplines. *Angew. Chem. Int. Ed.* 30, 34–38. doi: 10.1002/anie.199100341

Rakovan, J., Schmidt, G. R., Gunter, M., Nash, B., Kampf, A. R., Marty, J., et al. (2011). Hughesite, $Na_3Al(V_{10}O_{28})\bullet 22H_2O$, a new member of the pascoite family of minerals from the Sunday mine, San Miguel County, Colorado. *Can. Mineral.* 49, 1253–1265. doi: 10.3749/canmin.49.5.1253

Rao, A. S., Arumuganathan, T., Shivaiah, V., and Das, S. K. (2011). Polyoxometalates: toward new materials. *J. Chem. Sci.* 123, 229–239. doi: 10.1007/s12039-011-0115-2

Rehder, D. (2013). The future of/for vanadium. *Dalton Trans*. 42, 11749–11761. doi: 10.1039/c3dt50457c

Sánchez-Lombardo, I., Sánchez-Lara, E., Pérez-Benítez, A., Mendoza, Á., Bernès, S., and González-Vergara, E. (2014). Synthesis of metforminium(2+) decavanadates–crystal structures and solid-state characterization. *Eur. J. Inorg. Chem*. 2014, 4581–4588. doi: 10.1002/ejic.201402277

Sheldrick, G. M. (1997). *SHELX-97, Program for Crystal Structure Solution and Refinement.* Göttingen: University of Göttingen.

Vazylyev, M., Sloboda-Rozner, D., Haimov, A., Maayan, G., and Neumann, R. (2005). Strategies for oxidation catalyzed by polyoxometalates at the interface of homogeneous and heterogeneous catalysis. *Topics Catalysis* 34, 93–99. doi: 10.1007/s11244-005-3793-5

Villa, A. L., Vos, D. E. D., Verpoort, F., Sels, B. F., and Jacobs, P. A. (2001). A Study of V-pillared layered double hydroxides as catalysts for the epoxidation of terpenic unsaturated alcohols. *J. Catalysis* 198, 223–231. doi: 10.1006/jcat.2000.3104

Walsh, J. J., 1, Bond, A. M., Forster, R. J., and Keyes, T. E. (2016). Hybrid polyoxometalate materials for photo(electro-) chemical applications. *Coordination Chem. Rev*. 306, 217–234. doi: 10.1016/j.ccr.2015.06.016

Wang, M., Sun, W., Pang, H., Ma, H., Yu, J., Zhang, Z., et al. (2016). Tuning the microstructures of decavanadate-based supramolecular hybrids via regularly changing the spacers of bis(triazole) ligands. *J. Solid State Chem.* 235, 175–182. doi: 10.1016/j.jssc.2015.12.033

Winkler, P. A., Huang, Y., Sun, W., Juan Du,1, J., and Lü, W. (2017). Electron cryo-microscopy structure of a human TRPM4 channel. *Nature* 552, 200–204. doi: 10.1038/nature24674

Xie, F., Ma, F., Cui, S., Shu, G., Zhang, S., Tong Wang, T., et al. (2018). Synthesis and polypyrrole-loading study of antifungal medicine fluconazole functionalized Keggin polyoxotungstates. *J. Coordination Chem.* 71, 78–88. doi:10.1080/00958972.2018.1427234

Yerra, S., and Das, S. K. (2017). Organic free decavanadate based materials: inorganic linkers to obtain extended structures. *J. Mol. Struct.* 1146, 23–31. doi: 10.1016/j.molstruc.2017.05.097

Yi, Z., Yu, X., Xia, W., Zhao, L., Yang, C., Chen, Q., et al. (2010). Influence of the steric hindrance of organic amines on the supramolecular network based on polyoxovanadates. *CrystEngComm* 12, 242–249. doi: 10.1039/b916793p

Zhou, Y., Chen, G., Long, Z., and Wang, J. (2014). Recent advances in polyoxometalate-based heterogeneous catalytic materials for liquid-phase organic transformations. *RSC Adv.* 4, 42092–42113. doi: 10.1039/C4RA05175K

Conflict of Interest Statement: The authors declare that the research was conducted in the absence of any commercial or financial relationships that could be construed as a potential conflict of interest.